

ON THE LIKELIHOOD OF PLANET FORMATION IN CLOSE BINARIES

HANNAH JANG-CONDELL

University of Wyoming, Department of Physics & Astronomy
 1000 E. University, Dept 3905, Laramie, WY 82071

To Appear in The Astrophysical Journal

ABSTRACT

To date, several exoplanets have been discovered orbiting stars with close binary companions ($a \lesssim 30$ AU). The fact that planets can form in these dynamically challenging environments implies that planet formation must be a robust process. The initial protoplanetary disks in these systems from which planets must form should be tidally truncated to radii of a few AU, which indicates that the efficiency of planet formation must be high. Here, we examine the truncation of circumstellar protoplanetary disks in close binary systems, studying how the likelihood of planet formation is affected over a range of disk parameters. If the semimajor axis of the binary is too small or its eccentricity is too high, the disk will have too little mass for planet formation to occur. However, we find that the stars in the binary systems known to have planets should have once hosted circumstellar disks that were capable of supporting planet formation despite their truncation. We present a way to characterize the feasibility of planet formation based on binary orbital parameters such as stellar mass, companion mass, eccentricity and semi-major axis. Using this measure, we can quantify the robustness of planet formation in close binaries and better understand the overall efficiency of planet formation in general.

Subject headings: planets: formation — protoplanetary disks — binaries: close

1. INTRODUCTION

Close binary systems are a challenging environment for planet formation because a binary companion will dynamically perturb the protoplanetary disk. However, several exoplanets have been found in S-type orbits (circumstellar) around stars in binary systems with semi-major axes of less than 30 AU (e.g. Raghavan et al. 2006). These systems represent interesting test cases for planet formation theories. By comparing the frequency of planets in binary systems with that around single stars, we can learn about how robust the planet formation process can be. In this paper, we address the topic of circumstellar planets (S-type orbits), as opposed to circumbinary planets (P-type orbits).

HD 188753 is a hierarchical triple system, with a 12.3 AU separation and orbital eccentricity of 0.5 between the A and BC components. Konacki (2005) claimed the detection of planet around the A component. However, we found that the binary parameters for HD 188753A do not allow for in situ planet formation to occur (Jang-Condell 2007, henceforth Paper I). Indeed, it was later found that there was no planet there after all (Eggenberger et al. 2007).

On the other hand, γ Cep has a separation of 20 AU and eccentricity of 0.4, and has a well-established gas giant planet orbiting the A component at ~ 2 AU (Hatzes et al. 2003; Endl et al. 2011). Although at first glance, its orbit is not very different from that of HD 188753, we found that the binary parameters of γ Cep A do allow in situ planet formation to occur (Jang-Condell et al. 2008, henceforth Paper II).

Circumstellar planets have been discovered in a few other binary systems of comparable separations. These include HD 196885 (Correia et al. 2008; Fischer et al. 2009; Chauvin et al. 2011), α Cen (Pourbaix et al. 2002;

Dumusque et al. 2012; Hatzes 2013), and HD 41004. Interestingly, HD 41004 has substellar companions in both A and B components: HD 41004 Ab is a $2.5 M_J$ planet (Zucker et al. 2004) and HD 41004 Bb is a brown dwarf (Zucker et al. 2003). The binary orbits and planet characteristics of the systems discussed here are listed in Table 1.

One way to study the robustness of planet formation in binaries is to study the long-term dynamical stability of those planets Holman & Wiegert (e.g. 1999). However, the focus here in this work is on the formation of planets in the first place. Rather than doing a detailed calculation of the dynamics of planet formation as in, for example, Thebault (2011), we want to understand planet formation more broadly by considering the effects of binary interactions with the initial protoplanetary disk. That is, given that the protoplanetary disk will be truncated by a binary companion, what is the likelihood that planet formation can take place at all?

Calculations of disk truncation by binary companions show that stars in binary systems are still able to retain circumstellar disks (Artymowicz & Lubow 1994). This is supported by millimeter and submillimeter observations of pre-main sequence binaries which show that binary stars with separations of tens of AU are able to retain their disks (Jensen et al. 1996; Osterloh & Beckwith 1995; Jensen et al. 1994; Beckwith et al. 1990).

The objective of this paper is to give a measure for the difficulty of planet formation across a range of binary star parameters. We consider S-type orbits, in which the planet orbits one of the stars in the binary system, as opposed to P-type orbits, which refer to circumbinary planets. We examine the initial protoplanetary disk around a given star and calculate the degree of truncation of this disk. Rather than determining where exactly planets should form in these truncated disks, we focus on whether planet formation is possible at all.

TABLE 1
BINARY SYSTEMS ANALYZED IN THIS PAPER.

	HD 188753A	γ Cep A	HD 41004A	HD 41004B	HD 196885A	α Cen B
M_* (M_\odot)	1.06	1.40	0.7	0.4	1.31	0.93
M_b (M_\odot)	1.63	0.41	0.4	0.7	0.45	1.1
μ	0.39	0.77	0.64	0.36	0.74	0.46
a (AU)	12.3	20.2	20	20	21	23.5
e	0.5	0.41	0.4	0.4	0.42	0.52
$m_p \sin i$ (M_J)	—	1.85	2.5	18.4	2.96	0.0034
a_p (AU)	—	2.1	0.006	7×10^{-4}	2.6	0.04
e_p	—	0.05	0.7	0.08	0.46	0
reference	a	b	b,c	d	e	f
N_M	9	12	12	12	12	12
N_{DI}	0	1	1	1	1	1
N_{CA}	0	8	7	4	8	3

NOTE. — Orbital parameters without subscripts (a and e) refer to those of the binary. The subscript ‘p’ refers to planetary or substellar companions.

REFERENCES. — (a) Eggenberger et al. (2007), (b) Endl et al. (2011), (c) Zucker et al. (2004), (d) Zucker et al. (2003), (e) Correia et al. (2008), and (f) Dumusque et al. (2012)

In this paper, we extend the methods of determining the feasibility of planet formation in close binaries as developed in Papers I and II to a wider range of binary star configurations. For a given set of binary parameters, we develop a formalism for describing the feasibility of planet formation as measured by the number of disk models that would allow for either core accretion or disk instability to occur.

2. METHODS

2.1. Truncated Disk Models

We base our estimates of the likelihood of planet formation for a given binary system on the range of disk parameters that permit enough mass in the disk for planet formation to occur, given that a circumstellar protoplanetary disk will be truncated by a binary companion. These methods are explained fully in Papers I and II, and are summarized briefly here.

For convenience, we refer to the planet-hosting star as the primary and the binary stellar companion as the secondary, regardless of the relative masses between the binary components. Accordingly, M_* and M_b are the masses of the primary and secondary, respectively. The mass ratio of the binary is defined as $\mu = M_*/(M_* + M_b)$. The binary orbit is defined by the semimajor axis a , and eccentricity e .

The primary mass, M_* , affects both the gravitational potential of the disk as well as the amount of stellar irradiation of the disk since luminosity varies strongly with stellar mass. We consider a range of masses for the primary star from 0.5 to 2.0 M_\odot . To calculate the luminosity of the primary star, needed as an input parameter for the disk models, we use pre-main sequence models for stars of 1 Myr of age (Siess et al. 2000). The values for T_{eff} , R_* and L_* for each value of M_* selected are listed in Table 2.

The two additional parameters that determine the properties of a disk are the mass accretion rate (\dot{M}) and viscosity parameter (α). For each stellar mass, we calculate a suite of disk models by varying α and \dot{M} , as

$$\alpha \in \{0.001, 0.01, 0.1\} \quad (1)$$

and

$$\dot{M} \in \{10^{-9}, 10^{-8}, 10^{-7}, 10^{-6}, 10^{-5}, 10^{-4}\} M_\odot \text{ yr}^{-1} \quad (2)$$

TABLE 2
STELLAR PARAMETERS AS A FUNCTION OF STELLAR MASS

Stellar mass (M_\odot)	T_{eff} (K)	R_* (R_\odot)	L_*^\dagger (L_\odot)
0.5	3770	2.1	0.8
0.7	4026	2.4	1.4
0.9	4209	2.5	1.8
1.0	4282	2.6	2.0
1.1	4343	2.7	2.3
1.3	4447	2.9	3.0
1.5	4536	3.1	3.7
1.7	4616	3.3	4.4
1.9	4690	3.4	5.0
2.0	4721	3.5	5.5

† Derived from T_{eff} and R_* .

for a total of 18 disk models for each set of binary parameters (M_*, μ, a, e). The lower accretion rates reflect values typically observed in T Tauri disks. The highest accretion rates are more typical of active FU Orionis-like objects or very young protoplanetary disks than of passive T Tauri disks. Nevertheless, we include these high values of accretion for completeness.

A given value of α sets the viscosity, according to

$$\nu = \alpha c_s H \quad (3)$$

where c_s is the thermal sound speed and H is the scale height of the disk (Shakura & Sunyaev 1973). These quantities are related by $H = c_s \Omega$ where Ω is the Keplerian angular speed, and $c_s = \sqrt{kT/\bar{\mu}}$ where k is the Boltzmann constant, T is the midplane temperature, and $\bar{\mu}$ is the mean molecular weight of the gas, whose assumed composition is that of molecular hydrogen. The viscosity sets the rate of the mass flow through an accretion disk, according to

$$\nu \Sigma = \frac{\dot{M}}{3\pi} (1 - r/R_*) \quad (4)$$

where Σ is the surface density, r is the stellocentric radius, and R_* is the stellar radius (see, e.g., Pringle 1981). If we assume that the accretion rate, \dot{M} , is constant with r , then Eq. 4 gives a relation between T and Σ in the disk. Assuming that the only heating sources in the disk are viscous accretion and stellar illumination, we calculate

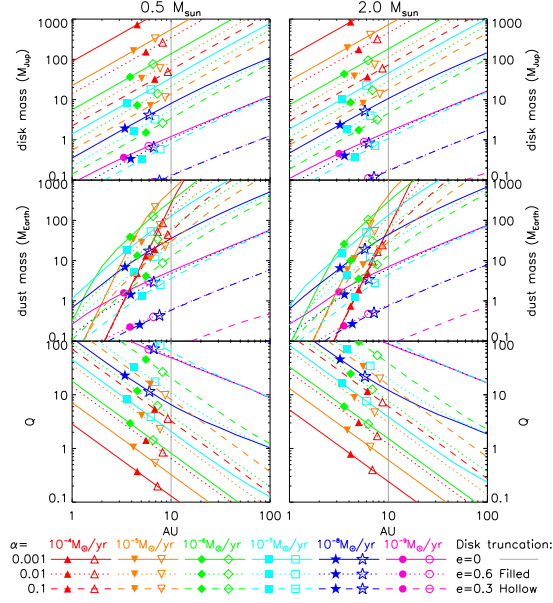


FIG. 1.— Disk profiles for the least massive ($0.5 M_{\odot}$, left) and most massive ($2.0 M_{\odot}$, right) planet host stars examined in this work. We show the total disk mass (top), total dust mass (middle), and Toomre Q parameter (bottom) versus radius for the disk parameters explored. The accretion rate (\dot{M}) is indicated by line color, while values of the viscosity parameter of $\alpha = 0.001, 0.01$, and 0.1 are indicated by solid, dotted, and dashed lines. The truncation radius for each disk for an equal-mass binary companion ($\mu = 0.5$) at $a = 30$ AU is shown by the vertical gray line for $e = 0$, by hollow symbols for $e = 0.3$ and filled symbols for $e = 0.6$.

$T(r)$ and $\Sigma(r)$ self-consistently. Thus, α and \dot{M} can be selected to “tune” the mass of the disk.

The truncation radius for each of the 18 disk models for a selected primary mass is determined from values calculated in Artymowicz & Lubow (1994), who define the truncation radius to be where viscous torques balance the tidal torques. This truncation radius depends both on the Reynolds number, which is controlled by the viscosity ν , and the binary orbit, represented by the mass ratio and eccentricity. That is, for each set of \dot{M} and α for the disk, and M_* , μ , a , and e for the binary, there is a unique disk truncation radius.

In Figure 1, we show how the structure of the disks vary with input parameters. The two sets of plots show disk profiles for the least massive ($0.5 M_{\odot}$) and most massive ($2.0 M_{\odot}$) stars explored. Each line represents a selected value of \dot{M} and α for a given disk model, as indicated by color and line type according to the legend. For each disk model, we show the enclosed disk mass (top), total dust mass (middle), and Toomre Q parameter (bottom) as a function of radius. The Toomre Q parameter is given by

$$Q = \frac{c_s \kappa}{\pi G \Sigma}, \quad (5)$$

where κ is the epicyclic frequency and G is the gravitational constant. Since the disk orbital velocities are close to Keplerian, we assume that $\kappa \approx \Omega$.

If the binary orbit is circular, then all disks will be truncated at the same radius. The truncation radius for an equal-mass binary companion ($\mu = 0.5$) at 30 AU in

a circular orbit is 10 AU, as indicated by a gray line in Figure 1. However, if the binary companion is eccentric, the truncation radius varies with disk properties. This is because the Reynolds number is different in each disk, therefore the balance of tidal and viscous torques occurs at different radii. The truncation radii for a binary orbit with $\mu = 0.5$ and $a = 30$ AU with $e = 0.3$ (0.6) is shown by hollow (filled) symbols in Figure 1. As the eccentricity increases, the truncation radii move inward as expected, since the periastron occurs at smaller radius with increasing eccentricity.

The disk profiles shown in Figure 1 vary more with \dot{M} and α than with stellar mass. As the stellar mass increases, the disks become slightly more massive overall, but with less dust and higher values of Q . This is because the increased stellar illumination heats the disks to higher temperature, which affects both disk sublimation and pressure support of the gas.

The Toomre Q parameter decreases with radius in most models of protoplanetary disks as a general rule. In the disk models presented, the midplane temperature and surface density typically behave as $T_c \propto r^{-0.6}$ and $\Sigma \propto r^{-0.9}$, respectively. Since $\Omega \propto r^{-3/2}$, the overall variation of Q is to decrease with r ,

2.2. Core Accretion vs. Disk Instability

Given a set of parameters defining a particular binary system (M_* , μ , a , and e), we can count how many of the 18 truncated disk models constructed around the primary star (1) have sufficient total mass to form planets, (2) have sufficient solid material to form a planet core, or (3) have low enough value of Q for disk instability to occur. If either condition (2) or (3) is satisfied, then (1) is also satisfied, so we henceforth consider only the more stringent criteria for planet formation based on core accretion and disk instability, rather than the total disk mass. We define the number of disks in which core accretion is possible based on the mass of solid material to be N_{CA} and the number of disks in which disk instability is possible based on the value of Q to be N_{DI} .

In the core accretion process of planet formation, giant planets are formed by first creating a rocky core from the agglomeration of dust particles in the disk. When it reaches sufficient mass, typically around $10 M_{\oplus}$, it becomes massive enough to accrete and retain a gaseous atmosphere, and gas giant planet is born. Our criterion for determining that a given truncated disk model is capable of forming giant planets by core accretion, then, is that it contains at least $10 M_{\oplus}$ of solid materials, i.e. dust and ice. If the total amount of dust in a given truncated disk model is above $10 M_{\oplus}$, then we say that that disk is capable of supporting planet formation by core accretion. So, N_{CA} is the total number of truncated disk models that can support planet formation by core accretion for a given set of binary parameters. For example, N_{CA} for $M_* = 0.5 M_{\odot}$, $\mu = 0.5$, $a = 30$ AU, and $e = 0$ can be read off the dust mass plot in Figure 1 (left center) by counting the number of profiles that intersect the truncation radius (gray line) at $10 M_{\oplus}$ or above, giving $N_{CA} = 12$. When the eccentricity is raised to $e = 0.3$, the solid content of the disk model with $\dot{M} = 10^{-6} M_{\odot} \text{ yr}^{-1}$ and $\alpha = 0.1$ drops below $10 M_{\oplus}$, so $N_{CA} = 11$.

The criterion for planet formation by disk instability,

on the other hand, is determined by the value of the Toomre instability parameter, Q . When $Q < 1$, the disk is gravitationally unstable and can rapidly form gas giant planets through fragmentation. If a given truncated disk model has $Q < 1$ at any point in the disk, then we declare that the disk is capable of forming planets by disk instability, and N_{DI} is the total number of truncated disk models that are gravitationally unstable for a given set of binary parameters. For $M_* = 0.5 M_\odot$, $\mu = 0.5$, $a = 30$ AU, and $e = 0$, $N_{\text{DI}} = 4$, and when the eccentricity is raised to $e = 0.3$ $N_{\text{DI}} = 3$.

3. RESULTS AND ANALYSIS

In Papers I and II, we used a fixed set of parameters for M_* , a , e , and μ and used those parameters to calculate N_{CA} and N_{DI} . Here, we extend the ranges of M_* , a , e , and μ in order to see how N_{CA} and N_{DI} vary with each parameter. In Table 1, we show our calculations for N_{CA} and N_{DI} for the binary systems listed there.

Our previous results for HD 188753A (Paper I) and γ Cep A (Paper II) are shown in the first two columns, respectively. We also repeat our calculations for the close binary systems HD 41004, HD 196885A, and α Cen B. Although HD 41004Bb is a brown dwarf rather than a planet, we include that system in this paper as a comparison.

HD 188753A, where there is no confirmed planet, is the only system with $N_{\text{DI}} = 0$; all other systems have $N_{\text{DI}} = 1$. Similarly, HD 188753A is the only system examined here with $N_{\text{CA}} = 0$. If we use N_{CA} as a proxy for the difficulty of planet formation, then α Cen B should be the least likely system to harbor a planet, and γ Cep A and HD 196885A the most likely.

In Figure 2 we show examples of how N_{CA} and N_{DI} vary with a and e , holding M_* and μ fixed. That is, the masses of the binary system are held fixed and their orbits are allowed to vary. One plot shows where γ Cep A falls in parameter space, while the other shows the location of HD 188753A. As eccentricity decreases and semi-major axis increases, N_{CA} (green solid contours) and N_{DI} (red dashed contours) both increase, as expected. This is because as periastron increases, the disk truncation radius also increases, allowing a larger disk to remain around the star. N_{DI} increases also because Q tends to decrease with increasing distance from the star, and N_{CA} increases because more cold disk material remains in the disk.

The irregularity in the spacing of the green contours (N_{CA}), particularly at large a and small e , results from the finite sampling of disk models. If we had included more values of \dot{M} and α , then there would be more contours in this area. Some of the contours bunch up at small separations and low eccentricities, largely because the solid content of the disks are not a simple function of \dot{M} and α , as shown in the middle panels of Figure 1. The dust mass versus radius profiles of the disks cross each other at small separations, with steeper profiles at higher accretion rates. This is because holding α constant, higher accretion rates give higher disk mass according to Equation (4), but the heating from this accretion causes sublimation of the refractory species. These competing effects mean that at large disk radii, the total solid content should overall be higher in the more massive, higher accretion rate disks, but at small radii, the

refractory species sublimate and those disks have lower solid content.

The values of N_{DI} and N_{CA} can be fit to a polynomial function dependent on a , e , μ , and M_* . The general form of this polynomial is

$$N = \sum_{i,j,k,l} c_{ijkl} \left(\frac{a}{1 \text{ AU}} \right)^i e^j \mu^k \left(\frac{M_*}{M_\odot} \right)^l. \quad (6)$$

Since we want to keep the analytic function as simple as possible, we do not try to fit the bunched contours, but rather try to find a smooth fit that will give a reasonable approximation for the true values of N_{CA} and N_{DI} . We find best-fitting polynomial coefficients, c_{ijkl} , for N_{CA} , using those points where they have tabulated values where $0 < N_{\text{CA}} \leq 10$, because this avoids the plateau in N_{CA} values at larger separations and low eccentricity. For N_{DI} , we use tabulated values where $0 < N_{\text{DI}} \leq 5$. As shown in Figure 2, values of N_{DI} higher than 5 occur only at $a \gtrsim 50$ AU and at low eccentricity, and in a region where $N_{\text{CA}} > 10$.

We find that for N_{CA} we get reasonably good fits for a function linear in a and e and quadratic in μ and M_* . For N_{DI} , the fitting function is linear in all four parameters. The best-fitting coefficients are tabulated in Table 3. Comparing the directly calculated and tabulated values for N_{CA} to the polynomial fit for all tabulated values where $N_{\text{CA}} \leq 10$, the root-mean-square deviation is 0.62. For $N_{\text{DI}} \leq 5$, the rms deviation is 0.44.

The values of N_{CA} and N_{DI} for the binary systems considered in this paper as calculated using this polynomial equation are tabulated in Table 4. Since both N_{CA} and N_{DI} cannot be less than 0, negative values should be interpreted as 0. The resulting values are all within ± 1 for N_{CA} , and within ± 0.6 for N_{DI} of the directly calculated values shown in Table 1. The polynomial values are more discrepant for larger values of N_{CA} , underestimating the true values. This is a result of the polynomial equation smoothing over the bunching of N_{CA} contours, as discussed above.

The values of N_{DI} for all binary systems considered are less than 2, as shown both in Table 1 and Table 4. This could be an indication that core accretion is more likely than disk instability in close binaries. As shown in Figure 1, the disk model with the lowest Q values has the highest accretion rate, $10^{-4} M_\odot \text{ yr}^{-1}$ and the lowest viscosity parameter explored. Disks with this high an accretion rate are typically outburst systems, such as FU Orionis objects. Accretion rates this high are typically transient. The disk contains $100 M_J$ or $0.1 M_\odot$ within just 1 AU, so it is extremely massive, hence it is the most gravitationally unstable. Because a steady-state disk with these properties is unlikely, planet formation via disk instability is also unlikely.

If we were to set a minimum threshold for N_{CA} for which planet formation can occur in a close binary given the binary systems explored in this paper, we first need to consider which systems to include. The existence of α Cen Bb has yet to be definitively confirmed, and it has the lowest value of N_{CA} of 3, not including HD 188753A. If α Cen Bb is confirmed, then we might set $N_{\text{CA,min}} = 3$. One might dispute that HD 41004Bb is a brown dwarf and ought not be considered, also. Then, we might set $N_{\text{CA,min}} = 7$, since γ Cep A, HD 41004A, and HD

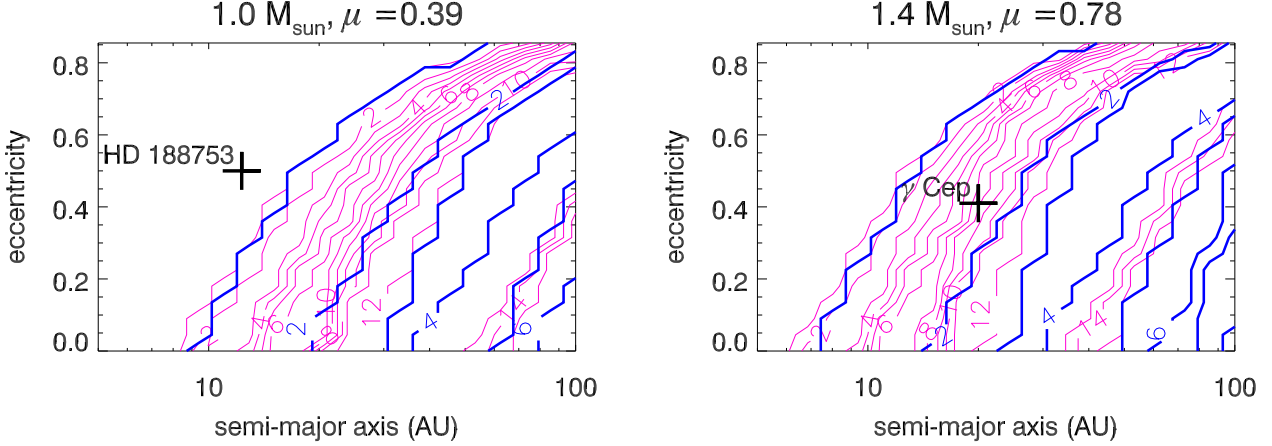


FIG. 2.— Planet formation likelihood plots for HD 188753A (left) and γ Cep A (right). Each plot shows how N_{CA} and N_{DI} vary with eccentricity and semi-major axis for the binary orbit for a fixed primary and secondary mass. Solid magenta contours show values for N_{CA} and dashed blue contours show those for N_{DI} . The positions of HD 188753A (left) and γ Cep A (right) in a - e space are indicated by crosses.

TABLE 3
COEFFICIENTS FOR EQUATION (6).

	$i = 0, j = 0$	$i = 1, j = 0$	$i = 0, j = 1$	$i = 1, j = 1$
Core Accretion				
$k = 0, l = 0$	-6.7585	0.4308	2.9369	-0.4411
$k = 1, l = 0$	-2.0956	1.6243	-9.5050	-1.4578
$k = 2, l = 0$	1.8452	-0.5589	16.0528	0.3879
$k = 0, l = 1$	1.5486	-0.1609	-1.9967	0.1696
$k = 1, l = 1$	-9.3964	0.2216	3.5221	-0.3374
$k = 2, l = 1$	7.9117	-0.3244	-5.4470	0.4971
$k = 0, l = 2$	-0.2951	0.0364	0.4372	-0.0363
$k = 1, l = 2$	2.7651	-0.0993	-1.6003	0.1275
$k = 2, l = 2$	-2.2214	0.0920	2.1346	-0.1406
Disk Instability				
$k = 0, l = 0$	0.3921	0.0521	-0.8329	-0.0431
$k = 1, l = 0$	-0.1135	0.1106	1.1926	-0.0975
$k = 0, l = 1$	-0.2704	-0.0066	0.3131	0.0012
$k = 1, l = 1$	0.2944	-0.0296	-0.7153	0.0327

TABLE 4
CALCULATED VALUES OF N_{CA} AND N_{DI} FROM EQUATION (6).

	HD 188753	γ Cep	HD 41004A	HD41004B	HD 196885	α CenB
N_{DI}	0.54	1.41	1.57	1.25	1.45	1.15
N_{CA}	-2.19	7.04	6.87	3.83	7.13	3.45

196885A all satisfy this criterion. Setting $N_{CA,min} = 7$ is the more stringent constraint for planet formation, since we require more disks to satisfy the requirement for sufficient solid mass. Based on these considerations, we predict that $N_{CA} \gtrsim 7$ for planet formation to be readily feasible, based on the known planets in binary systems. For $3 < N_{CA} < 7$, planet formation may still be possible, as in α Cen A, but less common.

In Figure 3, we show the allowed parameter space for planet formation in close binaries, with $N_{CA,min} = 3$ (left) or $N_{CA,min} = 7$ (right). That is, we set equation (6) equal to 3 or 7, choose fixed values of M_* and μ , and draw the resulting curve in a - e space. Since equation (6) is linear in a and e , the resulting curve for $N = N_{CA,min}$

is hyperbolic in a - e space for fixed M_* and μ .

For a given binary pair, giant planet formation by core accretion is allowed for greater separations and lower eccentricity than the indicated contour, or under each curve. Planet formation also becomes more feasible as the primary mass decreases and the mass ratio increases, as shown by the shifting of the contours up and to the left.

Note that for $a = 12$ AU, the semi-major axis of the HD 188753 binary, planet formation is highly disfavored. Even considering $N_{CA,min} = 3$, only stars with relatively low-mass companions ($\mu \gtrsim 0.7$ or $M_b/M_* \lesssim 3/7$) and low eccentricity ($e \lesssim 0.5$) might allow planet formation to occur. However, for $a = 20$ AU, a large range of binary

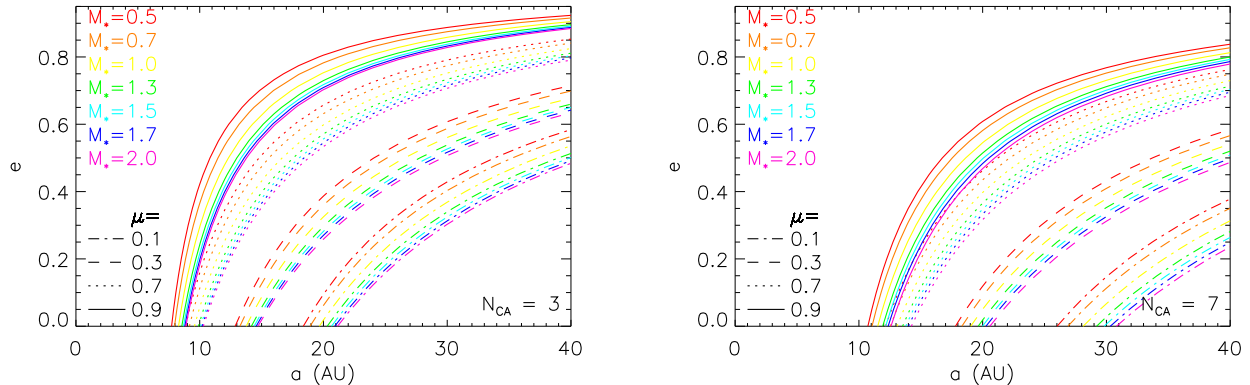


FIG. 3.— Contours in a - e space for $N_{\text{CA}} = 3$ (left) and $N_{\text{CA}} = 7$ (right) for varying binary masses. Each contour represents a selected choice for M_* and μ , and the axes show allowed values of a and e . The mass of the primary star is labeled by color, and the mass ratio of its binary companion is indicated by line style: dot-dashed, dashed, dotted, and solid for $\mu = 0.1, 0.3, 0.7$, and 0.9 , respectively. Planet formation becomes more feasible to the right and below each curve.

properties allow for planet formation to occur, although larger values of μ are favored.

4. DISCUSSION AND CONCLUSIONS

We have calculated the feasibility of giant planet formation in the close binary systems HD 188753, γ Cep, HD 41004, HD 196885, and α Cen. We find that except for HD 188753, where there is not a planet, core accretion is the more likely planet formation mechanism than disk instability based on simple models of the truncated protoplanetary disk from which the planet formed. These truncated disks contain a sufficiency of solid material from which planet cores can form, but do not meet the criterion for gravitational instability. Based on the results for these systems, we conclude that for binary systems of separations $\lesssim 20$ AU and eccentricity $\gtrsim 0.4$, circumstellar giant planets may only form via core accretion.

More generally, we extend our results to binary systems of arbitrary masses, separations, and eccentricities to predict the likelihood of giant planet formation by either core accretion or disk instability. These likelihoods are represented by the quantities N_{CA} and N_{DI} , respectively. We find an empirical fit to N_{CA} and N_{DI} as a function of binary mass, mass ratio, separation. By comparing N_{CA} and N_{DI} as predicted in this paper to the observed frequency of planets in binaries, we can gain insight into the planet formation process in general.

The estimates of planet formation likelihood represented by N_{CA} and N_{DI} are not meant to be definitive relations for the probability of planet formation. Rather, these values should be used to represent the relative ease with which planet formation can take place in binary systems. As more planets are found in close binary systems, those statistics can be compared to the likelihoods calculated in this work to yield a better understanding of how planets can form in the dynamically challenging environment of a close binary star.

We have considered only giant planet formation. In principle, the requirement for terrestrial planet formation is less stringent, since less solid material is required. These calculations would be a possible direction for future work.

Our results have been calculated under the assumption

that the circumstellar disk is coplanar with the binary orbit. It is conceivable that the disk could be misaligned with the binary, as is the case for the wide pre-main sequence binary HK Tau (Jensen & Akeson 2014). However, tidal effects from close stellar companions with $\lesssim 20$ AU separations will probably cause the disk to become aligned. The orbits of circumbinary planets discovered by the Kepler mission are closely aligned with those of the binary, suggesting that disks are likely to be aligned with binary orbits (Doyle et al. 2011; Welsh et al. 2012; Orosz et al. 2012b,a).

We have made the assumption in the core accretion case that likelihood of planet formation depends only on the total solid mass being above a certain threshold, and that it does not depend on the amount above that threshold. We do not calculate whether or not these solids can come together to form a single core, nor do we consider the possibility of the formation of multiple cores. These types of calculation would involve detailed modeling of the dynamics of the particles within the disk, and is beyond the scope of this paper.

We also do not consider the growth and evolution of giant planets within the disk beyond the initial formation. Dynamical effects such as tidal torques on planetesimals and planet embryos, planet-planet scattering, and disk migration will affect the survivability of planets within the system. These effects have been considered in some individual systems by others (e.g. Thebault 2011).

We have not considered how metallicity or chemical composition of the disk might affect our results. Increased metallicity will affect both the disk opacities and the amount of solids in the disks. Qualitatively speaking, increased opacity will result in slightly higher disk temperatures, which will decrease the refractory content in the most severely truncated disks. On the other hand, higher metallicity will raise the refractory content overall, so these effects will compete with each other. This could result in a lower likelihood of giant planet formation in the most tightly bound binary systems, but increased likelihood in wider systems.

Thanks go to Eric Jensen and an anonymous referee for helpful comments that greatly improved this paper. The author acknowledges support from NASA ATP Grant

NNX12AD43G.

REFERENCES

- Artymowicz, P. & Lubow, S. H. 1994, *ApJ*, 421, 651
- Beckwith, S. V. W., Sargent, A. I., Chini, R. S., & Guesten, R. 1990, *AJ*, 99, 924
- Chauvin, G., Beust, H., Lagrange, A.-M., & Eggenberger, A. 2011, *A&A*, 528, A8
- Correia, A. C. M., Udry, S., Mayor, M., Eggenberger, A., Naef, D., Beuzit, J.-L., Perrier, C., Queloz, D., Sivan, J.-P., Pepe, F., Santos, N. C., & Ségransan, D. 2008, *A&A*, 479, 271
- Doyle, L. R., Carter, J. A., Fabrycky, D. C., Slawson, R. W., Howell, S. B., Winn, J. N., Orosz, J. A., Prša, A., Welsh, W. F., Quinn, S. N., Latham, D., Torres, G., Buchhave, L. A., Marcy, G. W., Fortney, J. J., Shporer, A., Ford, E. B., Lissauer, J. J., Ragozzine, D., Rucker, M., Batalha, N., Jenkins, J. M., Borucki, W. J., Koch, D., Middour, C. K., Hall, J. R., McCauliff, S., Fanelli, M. N., Quintana, E. V., Holman, M. J., Caldwell, D. A., Still, M., Stefanik, R. P., Brown, W. R., Esquerdo, G. A., Tang, S., Furesz, G., Geary, J. C., Berlind, P., Calkins, M. L., Short, D. R., Steffen, J. H., Sasselov, D., Dunham, E. W., Cochran, W. D., Boss, A., Haas, M. R., Buzasi, D., & Fischer, D. 2011, *Science*, 333, 1602
- Dumusque, X., Pepe, F., Lovis, C., Ségransan, D., Sahlmann, J., Benz, W., Bouchy, F., Mayor, M., Queloz, D., Santos, N., & Udry, S. 2012, *Nature*, 491, 207
- Eggenberger, A., Udry, S., Mazeh, T., Segal, Y., & Mayor, M. 2007, *A&A*, 466, 1179
- Endl, M., Cochran, W. D., Hatzes, A. P., & Wittenmyer, R. A. 2011, in *American Institute of Physics Conference Series*, Vol. 1331, American Institute of Physics Conference Series, ed. S. Schuh, H. Drechsel, & U. Heber, 88–94
- Fischer, D., Driscoll, P., Isaacson, H., Giguere, M., Marcy, G. W., Valenti, J., Wright, J. T., Henry, G. W., Johnson, J. A., Howard, A., Peek, K., & McCarthy, C. 2009, *ApJ*, 703, 1545
- Hatzes, A. P. 2013, *ApJ*, 770, 133
- Hatzes, A. P., Cochran, W. D., Endl, M., McArthur, B., Paulson, D. B., Walker, G. A. H., Campbell, B., & Yang, S. 2003, *ApJ*, 599, 1383
- Holman, M. J. & Wiegert, P. A. 1999, *AJ*, 117, 621
- Jang-Condell, H. 2007, *ApJ*, 654, 641
- Jang-Condell, H., Mugrauer, M., & Schmidt, T. 2008, *ApJ*, 683, L191
- Jensen, E. L. N. & Akeson, R. 2014, *Nature*, 511, 567
- Jensen, E. L. N., Mathieu, R. D., & Fuller, G. A. 1994, *ApJ*, 429, L29
- . 1996, *ApJ*, 458, 312
- Konacki, M. 2005, *Nature*, 436, 230
- Orosz, J. A., Welsh, W. F., Carter, J. A., Brugamyer, E., Buchhave, L. A., Cochran, W. D., Endl, M., Ford, E. B., MacQueen, P., Short, D. R., Torres, G., Windmiller, G., Agol, E., Barclay, T., Caldwell, D. A., Clarke, B. D., Doyle, L. R., Fabrycky, D. C., Geary, J. C., Haghighipour, N., Holman, M. J., Ibrahim, K. A., Jenkins, J. M., Kinemuchi, K., Li, J., Lissauer, J. J., Prša, A., Ragozzine, D., Shporer, A., Still, M., & Wade, R. A. 2012a, *ApJ*, 758, 87
- Orosz, J. A., Welsh, W. F., Carter, J. A., Fabrycky, D. C., Cochran, W. D., Endl, M., Ford, E. B., Haghighipour, N., MacQueen, P. J., Mazeh, T., Sanchis-Ojeda, R., Short, D. R., Torres, G., Agol, E., Buchhave, L. A., Doyle, L. R., Isaacson, H., Lissauer, J. J., Marcy, G. W., Shporer, A., Windmiller, G., Barclay, T., Boss, A. P., Clarke, B. D., Fortney, J., Geary, J. C., Holman, M. J., Huber, D., Jenkins, J. M., Kinemuchi, K., Kruse, E., Ragozzine, D., Sasselov, D., Still, M., Tenenbaum, P., Uddin, K., Winn, J. N., Koch, D. G., & Borucki, W. J. 2012b, *Science*, 337, 1511
- Osterloh, M. & Beckwith, S. V. W. 1995, *ApJ*, 439, 288
- Pourbaix, D., Nidever, D., McCarthy, C., Butler, R. P., Tinney, C. G., Marcy, G. W., Jones, H. R. A., Penny, A. J., Carter, B. D., Bouchy, F., Pepe, F., Hearnshaw, J. B., Skuljan, J., Ramm, D., & Kent, D. 2002, *A&A*, 386, 280
- Pringle, J. E. 1981, *ARA&A*, 19, 137
- Raghavan, D., Henry, T. J., Mason, B. D., Subasavage, J. P., Jao, W.-C., Beaulieu, T. D., & Hambly, N. C. 2006, *ApJ*, 646, 523
- Shakura, N. I. & Sunyaev, R. A. 1973, *A&A*, 24, 337
- Siess, L., Dufour, E., & Forestini, M. 2000, *A&A*, 358, 593
- Thebault, P. 2011, *Celestial Mechanics and Dynamical Astronomy*, 111, 29
- Welsh, W. F., Orosz, J. A., Carter, J. A., Fabrycky, D. C., Ford, E. B., Lissauer, J. J., Prša, A., Quinn, S. N., Ragozzine, D., Short, D. R., Torres, G., Winn, J. N., Doyle, L. R., Barclay, T., Batalha, N., Bloemen, S., Brugamyer, E., Buchhave, L. A., Caldwell, C., Caldwell, D. A., Christiansen, J. L., Ciardi, D. R., Cochran, W. D., Endl, M., Fortney, J. J., Gautier, III, T. N., Gilliland, R. L., Haas, M. R., Hall, J. R., Holman, M. J., Howard, A. W., Howell, S. B., Isaacson, H., Jenkins, J. M., Klaus, T. C., Latham, D. W., Li, J., Marcy, G. W., Mazeh, T., Quintana, E. V., Robertson, P., Shporer, A., Steffen, J. H., Windmiller, G., Koch, D. G., & Borucki, W. J. 2012, *Nature*, 481, 475
- Zucker, S., Mazeh, T., Santos, N. C., Udry, S., & Mayor, M. 2003, *A&A*, 404, 775
- . 2004, *A&A*, 426, 695